Supplemental Digital Content 1

Techniques adopted for measurement of the effect of auranofin on $CD4^+$ T-cell phenotype and viability.

Cell separation and isolation of $CD4^+$ T-cell subsets by cell sorting. Human PBMCs were isolated from whole blood by Ficoll centrifugation and resuspended in RPMI/10% foetal bovine serum (FBS). $CD4^+$ T-cells were isolated by negative selection on a Robosep (Stemcell, Vancouver, BC, Canada). Isolated $CD4^+$ T-cells (purity: >90%) were stained for 20 minutes at 4°C in PBS-4%FBS buffer with the following combination of antibodies: CD3-PB [Becton Dickinson (BD), Franklin Lakes, NJ], CD4-A700 (BD), CD45RA-ECD (Beckman Coulter, Brea, CA), CD27-Qdot655 (Invitrogen, Carlsbad, CA), CCR7-PE Cy7 (BD), Vivid-AmCyan (Invitrogen). Cell were washed in PBS-4% FBS before being resuspended at 30.10^6 cells per mL in the same buffer for sorting. Naïve $CD4^+$ T-cells (T_N), T_{CM}, T_{TM} and T_{EM} (purity: >98%) were sorted on an ARIA II (BD) at low pressure.

Cell cultures. Total $CD4^+$ T-cells and isolated subsets were cultured at $1x10^6$ cells/ml in RPMI supplemented with 10% FBS for two days in the presence of increasing concentrations of auranofin ranging from 0 to 500 nM.

Flow cytometry. After two days of culture, cells were harvested and stained for memory and activation markers using the following combination of antibodies and reagents: CD3-PB (BD), CD4-A700 (BD), CD45RA-APC H7 (BD), CD27-FITC (BD), CCR7-PE (R&D Systems, Minneapolis, MN), HLA-DR-PerCP (BD), Vivid-AmCyan (Invitrogen), Annexin V-APC (BD). Cells were stained for 20 minutes at 4°C in PBS-4%FBS buffer, and washed in PBS-4% FBS before being fixed in PBS-2%PFA before acquisition. 200,000 events were collected during flow cytometric analysis on a LSRII (BD Biosciences) and analyzed using the FlowJo software (Tree Star, Inc.).

Supplemental Digital Content 2

Additional Figures

Figure 1 of Supplemental Digital Content 2. Schematic representation of the animal experiments performed in the present study.

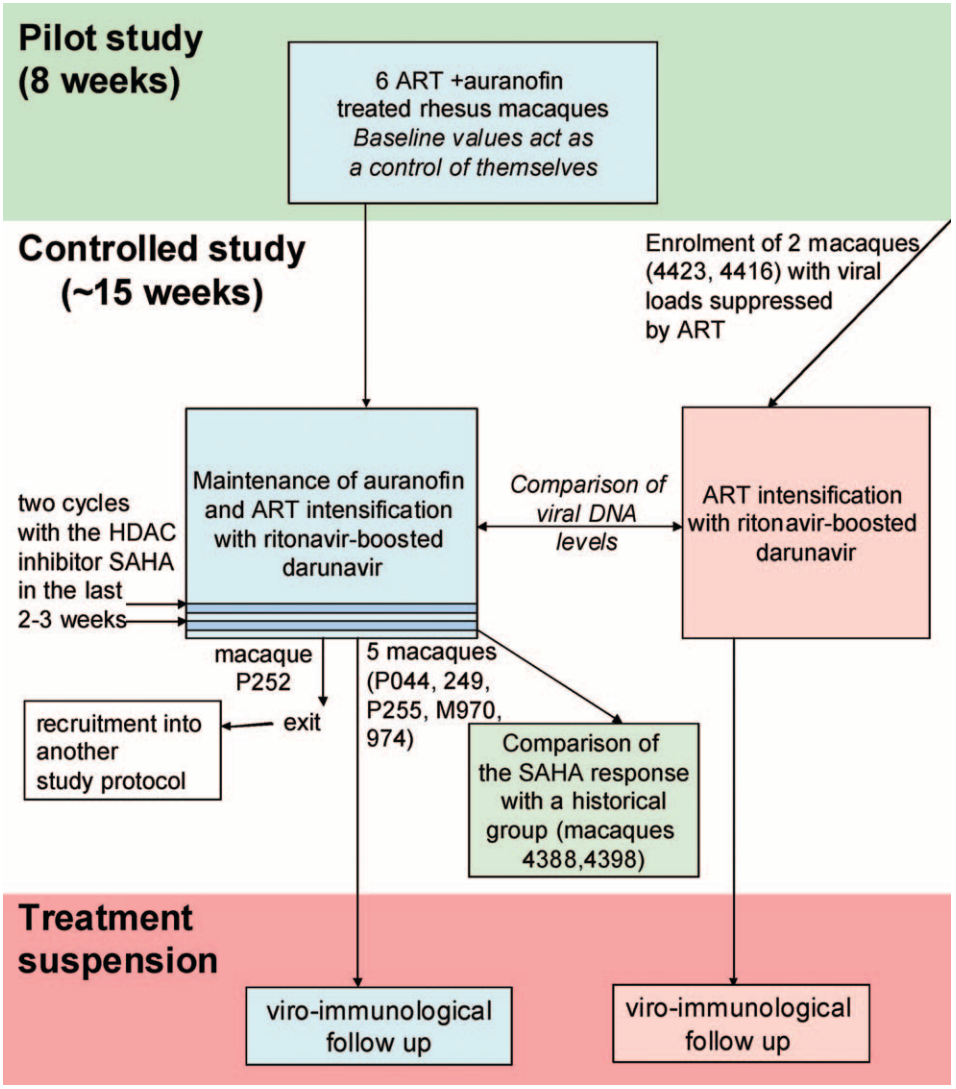

We initially conducted a pilot study aimed at evaluating the potency of auranofin to deplete the lentiviral reservoir in a recently published animal model, *i.e.* SIVmac251-infected rhesus macaques with VLs stably suppressed by three-drug ART (tenofovir+emtricitabine+raltegravir) [1].

This pilot study prompted us to evaluate the long-term effects of auranofin on viral DNA in a controlled study. As a control group, we enrolled two rhesus macaques with stably suppressed viremia under the same ART protocol adopted in the auranofin group. To prevent a possible viral reservoir reseeding through ongoing viral replication in anatomical compartment(s), ART was intensified with ritonavir-boosted darunavir in all animals.

In order to show the impact of auranofin plus iART on replication-competent viral reservoirs, we performed a dynamic test using the potent HDAC inhibitor, vorinostat (SAHA), endowed with antilatency/viral-replication enhancing activity [2,3]. Monkeys at week 10 of iART/auranofin treatment were treated with an oral dose of SAHA of 178.5 mg/m^2 of body surface twice daily for three days, and response was compared with that of two historical controls (*i.e.* subjects 4438

and 4398) that had received the same dosage of SAHA while being treated with the same iART protocol in the absence of auranofin.

The choice for comparing the SAHA response of the auranofin group with two historical controls was derived from ethical reasons, because the main financial sponsor of the present study (Fondazione Roma) specifically required that we not knowingly harm the macaques. Since the iART-only treated macaques 4388 and 4398 had previously shown loss of control of the infection upon administration of SAHA, we could not treat the iART-only controls of the present study with the same protocol. Instead, SAHA treatment was applied to the auranofin-plus-iART group because the significant decrease in viral DNA represented a strong indication for a decreased size of the viral reservoir, and, therefore, a reasonable limitation of the potential effect of SAHA on VL induction.

Finally, to test the capacity of auranofin to induce a natural long-term control of SIVmac251 replication in the absence of iART, all treatments were suspended and viro-immunological parameters were monitored periodically.

1. Lewis MG, Norelli S, Collins M, Barreca ML, Iraci N, Chirullo B, et al. Response of a simian immunodeficiency virus (SIVmac251) to raltegravir: a basis for a new treatment for simian AIDS and an animal model for studying lentiviral persistence during antiretroviral therapy. *Retrovirology* 2010; **7**:21.
2. Archin NM, Keedy KS, Espeseth A, Dang H, Hazuda DJ, Margolis DM. Expression of latent human immunodeficiency type 1 is induced by novel and selective histone deacetylase inhibitors. *AIDS* 2009; **23**:1799-806.
3. Savarino A, Mai A, Norelli S, El Daker S, Valente S, Rotili D, et al. "Shock and kill" effects of class I-selective histone deacetylase inhibitors in combination with the glutathione synthesis inhibitor buthionine sulfoximine in cell line models for HIV-1 quiescence. *Retrovirology* 2009; **6**:52.

Figure 2 of Supplemental Digital Content 2. Phenotypes of sorted $CD4^+$ naïve T-cells (T_N), $CD4^+$ central memory T-cells (T_{CM}), and $CD4^+$ transitional memory T-cells (T_{TM}) treated with auranofin (Aur) for 48 h. To confirm the pro-differentiating effect of auranofin, we sorted the $CD4^+$ T-naïve (T_N; *i.e.* $CD45RA^+CD27^+CCR7^+$), T_{CM} ($CD45RA^-CD27^+CCR7^+$), T_{TM} ($CD45RA^-CD27^+CCR7^-$) and T_{EM} ($CD45RA^-CD27^-CCR7^-$) subpopulations from enriched human $CD4^+$ T-cell fractions, and treated them with auranofin at 250 and 500 nM (Aur 250; Aur 500). The cells originally obtained by sorting and subjected to the treatments are indicated as parent cells (*x* axis). The corresponding proportions of the T-cell subsets that were obtained after two days of treatment are shown by the ordinate. One experiment out of three with similar results. The majority of cells displaying the $CD45RA^+CD27^{low/-}CCR7^+$ and $CD45RA^-CD27^{low/-}CCR7^+$ phenotypes are Annexin V^+ at 48 h and likely represent abortive or short-lived phenotypes (see Figure 3 of supplemental Digital Content 2; and data not shown). A consistently smaller portion of the untreated cells (which is donor-dependent; data not shown) also differentiate towards a $CD27^{low/-}CCR7^+$ phenotype.

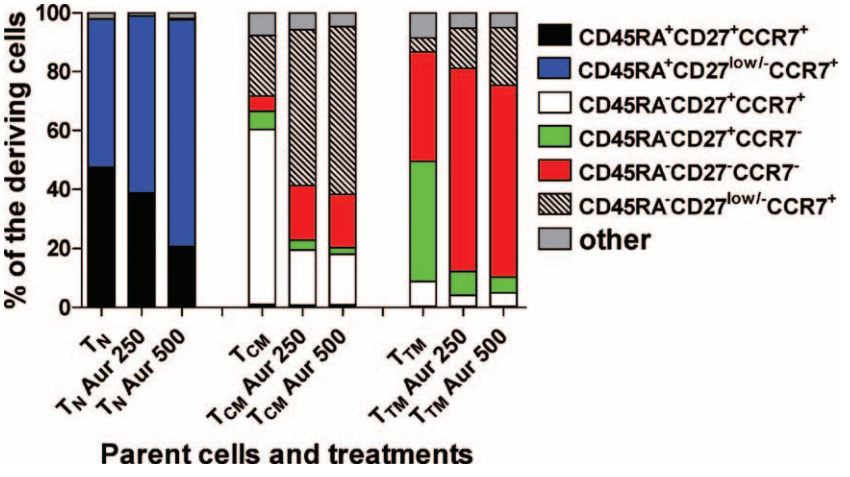

Figure 3 of Supplemental Digital Content 2. Dot plots showing anti-CD27 and annexin V staining at different time points during treatment with auranofin (gate on live cells). $CD4^+$ T-naïve (T_N), central memory (T_{CM}), and transitional memory (T_{TM}) cells were separated by sorting and treated with auranofin at 500 nM (Aur 500) or left untreated. Results show that auranofin induced CD27 downmodulation (*y* axis), which preceded Annexin V stainability (*x* axis). While the majority, if not all, of the cells from the memory compartment displayed the auranofin-induced changes, a significant proportion of naïve cells remained Annexin V^- at 48 h of culture. One representative experiment out of three with similar results. This experiment was performed using $CD4^+$ T-cells from a human subject different from the donor of cells used in the experiment of Figure 2 of Supplemental File 2.

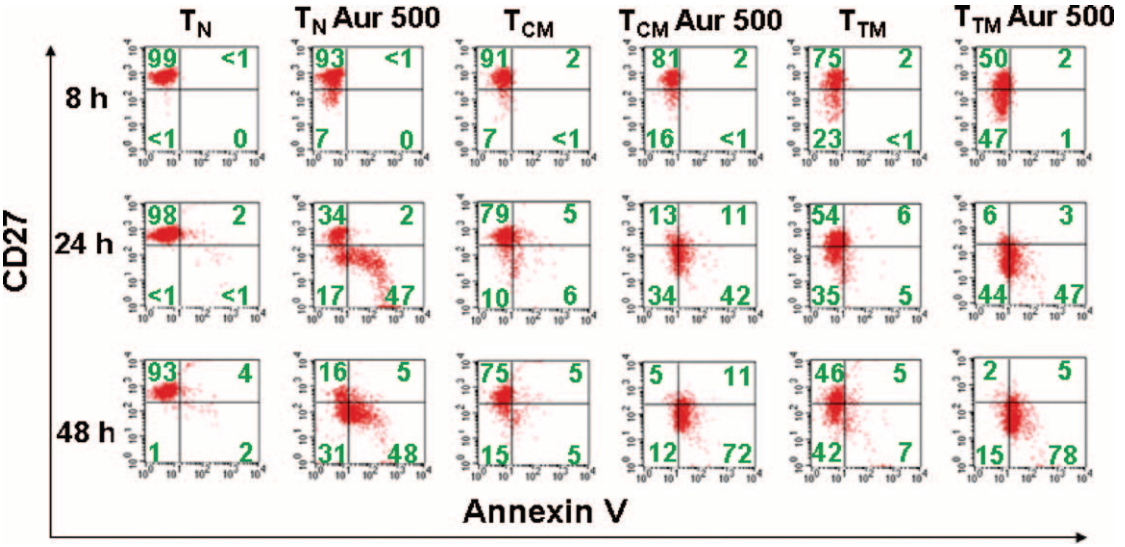

Figure 4 of Supplemental Digital Content 2. Auranofin treatment delays viral rebound upon treatment interruption. Data are presented as survival curves. Dotted lines delimit the 95% confidence intervals. The *P* value refers to the possibility of randomly choosing groups with timings of VL rebounds as different.

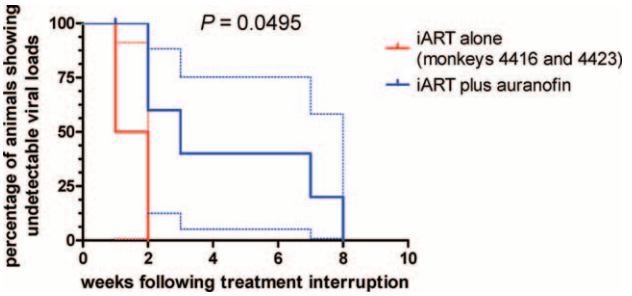

Figure 5 of Supplemental Digital Content 2. General trends of the ratio between the $CD4^+$ and $CD8^+$ T-lymphocyte absolute numbers (CD4/CD8 ratio) and $CD8^+$ T-lymphocyte absolute numbers (CD8 counts) following therapy suspension. A) CD4/CD8 ratio following therapy suspension in iART alone-treated macaques (two subjects, red) and auranofin plus iART-treated macaques (five subjects, blue). B) CD8 counts in the same groups as in panel A, *i.e.* the iART alone-treated macaques (two subjects, red) and auranofin plus iART-treated macaques (five subjects, blue). Means ± SEM are shown. The trends were calculated by a polynomial regression model, and the significance of the difference between the two groups' trends (shown on top of each panel) was calculated by the *F* test for comparison of regression curves. The trends in individual monkeys and the individual data points for the absolute numbers of $CD4^+$ and $CD8^+$ T-lymphocytes are shown in Figure 4. In A, the high SEM values in the iART-only controls are due to the fact that these moneys showed either a CD4/CD8 ratio which remained constantly subnormal, or CD8 counts decreasing in parallel with $CD4^+$ T-cells (see Fig. 4A of main text).

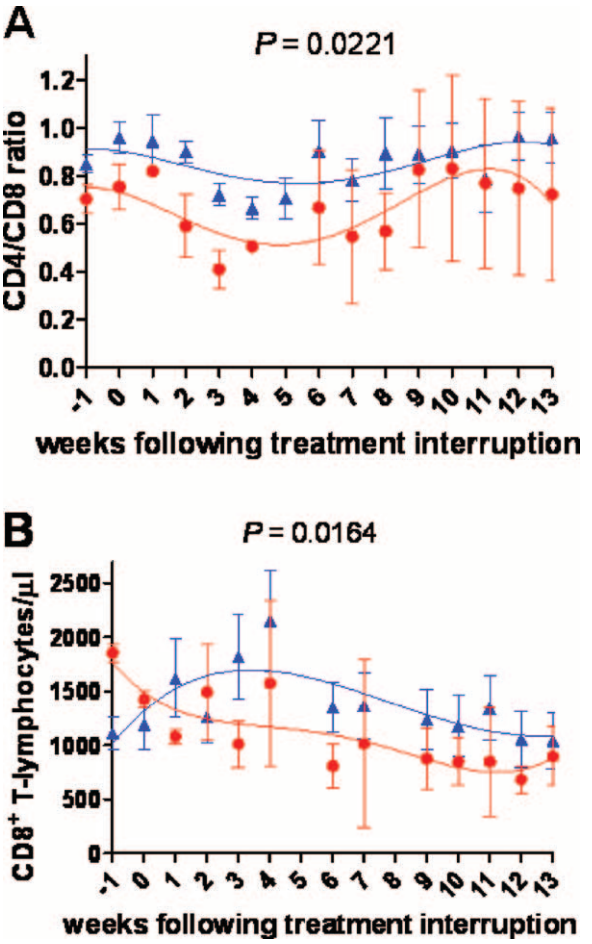

Figure 6 of Supplemental Digital Content 2. $CD4^+$ T-cell depletion upon ART interruption is negatively correlated with the frequency of cells harboring viral DNA. iART alone-treated animals are shown in red. Auranofin plus iART-treated animals are shown in different gradations of blue depending on the steepness of the slopes of CD4 counts following therapy suspension [top: non-significant or significantly positive slopes; bottom: significantly decreasing CD4 counts (negative slopes)]. Dashed curves represent the 95% confidence intervals.

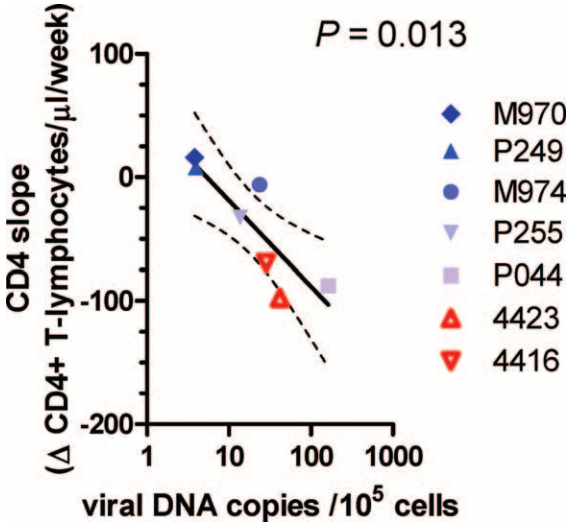

Supplemental Digital Content 3

Statistical analyses

Statistical analyses were conducted using GraphPad Prism, v5.0 (GraphPad software, La Jolla, CA), unless otherwise specified. Correlation between two variables was analyzed using Pearson's correlation coefficients (*r*), followed by the *t*-test for correlation. Multiple correlation was conducted using SPSS 15.0 for Windows (IBM SPSS, Chicago, IL). The number of animals enrolled in the pilot study was determined by the β-error calculator in the DSS Research website. Differences between variables were analyzed using parametric tests such as *t*-tests, or, in case of multiple comparisons, one- or two-way analysis of variance (ANOVA). Welch's correction was adopted where necessary. Paired or repeated-measures tests were adopted for matched observational data points. An appropriate transformation was done to restore normality, where necessary. The times to VL rebounds were analyzed by the non-parametric Gehan-Breslow-Wilcoxon test. P252 which was addressed to another study protocol before therapy suspension (Figure 1, Supplemental Digital Content 2) weighed as "censored" in the survival curve. Trends were analyzed by linear or non-linear regression. The simplest equation for which the fit converged was chosen. vRNA and vDNA set points following rebound were calculated as a geometric mean of all VLs available since three weeks after the VL peak. Initial exposure to the virus during viral rebound was estimated by calculating the area under curve of the VL peak.